Communications in Physics, Vol. 33, No. 1 (2023), pp. 51-62
DOI: https://doi.org/10.15625/0868-3166/17301

In silico study of the influences of cooling rates on the phase transition of water inside the carbon nanotube under different ambient pressures

Vi Toan Lam[1,2], **Giang Hoang Nguyen**[1,2], **Hoa Van Nguyen**[1,2], **Phi Minh Nguyen**[1,2] **and Hanh Thi Thu Tran**[1,2,†]

[1]*Laboratory of Computational Physics, Faculty of Applied Science, Ho Chi Minh City University of Technology (HCMUT), Ho Chi Minh City, 268 Ly Thuong Kiet Street, District 10, Ho Chi Minh City, Vietnam*

[2]*Vietnam National University Ho Chi Minh City, Linh Trung Ward, Thu Duc District, Ho Chi Minh City, Vietnam*

E-mail: [†]thuhanhsp@gmail.com

Received 6 July 2022

Accepted for publication 12 September 2022

Published 1 January 2023

Abstract. *By using the Molecular Dynamics simulation (MD) method, this study aims to show the influences of cooling rates on the solidifying temperature of the water inside a single-wall-carbon-nanotube (SWCNT) under different ambient pressures. We first created different systems with different tube diameters, then we cooled the systems from 300 K down to 200 K under different ambient pressures to observe the behavior of water. Our results showed that the more rapid cooling rate of the systems creates more disruptive and dramatic phase transitions that localize in specific ranges of temperature. Moreover, we also found that the lower pressures correlate to the more dramatic phase transitions of water molecules, regardless of the cooling rate. This study generally provides more insight into water behavior in the SWCNT with variations in ambient conditions.*

Keywords: single-wall-carbon-nanotube; water phase transition; cooling rates; pressures; MD simulation.

Classification numbers: 88.30.rh; 64.60.av.

1. Introduction

Water - one of the most abundant substances in our world, remains mysterious beyond our conventional knowledge. In 2017, the research team at Massachusetts Institute of Technology [1] shocked the world by discovering an unprecedented phenomenon in which water is frozen at and above its 100°C boiling point. That kind of unexpected behavior of water occurs due to the water molecules being confined in a small space. Thereby, the water molecules likely prevent the movement of each other when the temperature rises. Besides, there had been many previous studies that attempted to find out such anomalous behaviors of water. Koga and colleagues [2] were the first team to observe such a bizarre phase transition of water inside a single-wall-carbon nanotube (SWCNT) under high axial pressure above 50 MPa when cooling the system down below 300 K, using the MD simulation method. Walther *et al.* [3] also carried out the MD simulation to study the behavior of water transportation through SWCNT. Another research [4] investigated the continuous phase transition of ice molecules inside SWCNT where its melting curves show multiple local minima, which has not been observed in a phase transition of sole bulk water before. In addition, one research [5] also found that the water-water interaction is the main factor affecting the potential energy during the phase transition of water inside a carbon nanotube, whereas the carbon-water interaction affects the dependency of transition temperature on the tube diameter. The existence of ice in carbon nanotube was also discovered by experiment using the X-ray diffraction method [6, 7]. They observed that the water molecules begin to condense at around 315 K - 330 K, under saturated vapor pressure. The phase transition of water inside a carbon nanotube also depends on the ambient pressure. Jaeil Bai *et al.* [8] investigated the influence of pressure changes on the structure of solid ice at high temperatures. Another study [9] also found that at low pressures and room temperatures, the water molecules crystallized in carbon nanotube have a unique critical density, below which the ice structure starts to deform into the liquid state. That means the ice nanotube formation also depends on the density of water. Even at really low temperatures where the bulk water starts to form ice (at 0°C), the results proposed by Kolesnikov *et al.* [10] showed that the soft dynamics of water chains in the carbon nanotube causes the large mean-square displacement of water molecules as well as the drop in their freezing temperature. Furthermore, there exist controversial results among different experimental studies using the NMR method to find out the dependency of ice formation inside the SWCNT on water isotopes. One concluded that there is no difference when using different water isotopes [11], whereas another one [12] found out that the freezing temperatures are varied by different isotopes (i.e., the phase transition of water inside the 1.94 nm SWCNT was 220 K for H1 and 240 K for heavy water). Moreover, as verified by some research [1, 5], the solidification of water inside the SWCNT is strongly affected by the diameter of the tube, which is manifested in Ref. [1]. They also showed that when changing the diameter of the carbon nanotube from 10.5 Å to 10.6 Å ($\sim 1\%$ in ratio change), the freezing temperature of water dramatically drops from about 140°C down to 100°C. So in general, water exhibits bizarre properties in the presence of carbon nanotubes under different conditions. However, there is one factor that is rarely taken into account: the temperature changing rate. Previous research proposed that the different heating or cooling rates may cause huge changes in both phase transition points and post-transition structures of materials [5, 13–15]. Moreover, those changes may variate at different ambient pressures. This is our motivation to

carry out this study, to clarify how the phase transition of water is dually affected by different cooling rates with different ambient pressures.

2. Materials and methods

2.1. Modelling

We first created the carbon nanotube structure using the Nanotube Builder Package of VMD software [16]. We built three nanotube structures with three different diameters at the same lengths of 50 Å as shown in Fig. 1. Each diameter corresponds to each set of chiral indices (n,m) of the tube. For the diameter of 9.4 Å, the indices are (6,8); whereas for the diameters of 10.3 Å and 10.5 Å, the indices are (5,10) and (4,11), respectively. The reason we chose to build three tubes with small variations in diameters (1.1 Å at max) is due to the study mentioned above [1].

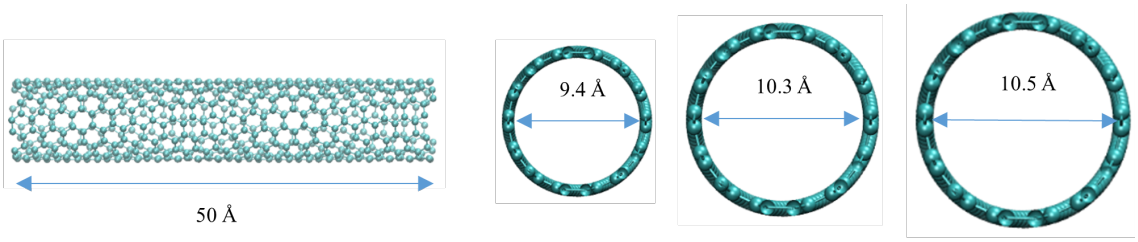

Fig. 1. Initial carbon nanotube models with three different diameters at the same length.

The tube structures are then solvated with water molecules using Packmol software [17]. We put 1000 molecules of water inside the simulation box of size (20×20×80) Å as shown in Fig. 2.

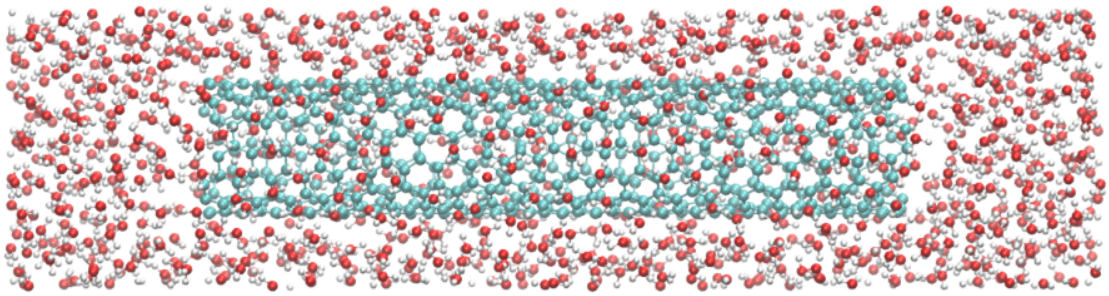

Fig. 2. (Color online) The solvation complex in simulation box of size (20×20×80) Å. The carbon, oxygen, and hydrogen atoms are depicted in blue, red, and white, respectively.

2.2. Simulation

The obtained complex structures were then carried to LAMMPS software to conduct the MD simulation. We chose the time step of 1 fs and the periodic boundary conditions for all simulation procedures. The water model used in this research is the TIP3P model modified for the CHARMM force field [18]. As for the carbon nanotube, we chose the AIREBO force field which well describes the interaction energy between carbon atoms [19]. The non-bonded interaction between carbon atoms and water molecules is described with CHARMM force field as well.

At the start of the simulation processes, we carried out the energy minimization for the whole system using the Conjugate Gradient method, which modifies the box size as well as the distance between the water molecules. That process purposely yields the stable state of the system. After that, we equilibrated the system using canonical ensemble NVT and isothermal-isobaric ensemble NPT with the Nose-Hoover thermostat and barostat. More specifically, the NPT process was divided into two parts. Firstly, the NVT and NPT processes were conditioned to the room temperature of 300 K under three different pressures of 1 bar, 0.5 bar, and 2 bar. Then, the second NPT process was used to cool down the system to 200 K under the same pressure conditions as the first NPT process but with three different cooling rates: 2×10^{11} K/s (fast), 5×10^{10} K/s (medium), 2×10^{10} K/s (slow). We summarized the conditions in Table 1.

Table 1. Summary of macrostate conditions used for simulation. Each simulation system corresponds to a set of three values in the table.

Pressure	0.5 bar
	1 bar
	2 bar
Cooling rate	2×10^{11} K/s
	5×10^{10} K/s
	2×10^{10} K/s
Tube diameter	9.4 Å
	10.3 Å
	10.5 Å

3. Results and discussion

3.1. Under normal pressure of 1 bar

At the first glance, we notice that there are different tendencies in the Mean-squared displacement (MSD) graphs above with different cooling rates (Fig. 3a - 3c). When using fast cooling rate, the formation of ice is inconsistent, until when the temperature reaches below 240 K that consistent ice structures are created. The decrease in cooling rate, as shown in Fig. 3b - 3c, leads to

the higher temperature of the critical transition point to form the consistent ice structures. At the slow cooling rate of 2×10^{10} K/s, the critical transition points of water inside the SWCNT are above 240 K for all three diameters of tubes, and are relatively more consistent compared with the faster cooling rates.

More detailed insight into the cooling progress is illustrated in Fig. 3 and Table 2. For the fast cooling rate systems, the heat capacity graph (Fig. 3d) shows the first prominent peaks around 280 K which illustrate the premature phase transition of water. Such existence of partial phase transition of water inside the SWCNT was also observed previously at higher temperature than 273 K [20]. The globally high peaks in the cases of 10.5 Å and 10.3 Å tubes indicate the ice structures majorly forming at 280 K. On the other hand, in the case of the 9.4 Å tube, multiple peaks demonstrate the continuously structural formation of the ice at temperatures above 230 K, and the consistent ice structure is created at an extremely low temperature, as described by the peaks below 230 K.

Table 2. Summary of the noticeable phase transition points of systems under 1 bar pressure.

Cooling rate (K/s)	Diameter (Å)	Temperature of first local peak (K)	Critical phase transition point (K)
2×10^{11} (fast)	9.4	290	230
	10.3	280	240
	10.5	280	240
5×10^{10} (med)	9.4	275	250 - 260
	10.3	260	240
	10.5	260	250
2×10^{10} (slow)	9.4	~ 300	250
	10.3	290	245
	10.5	280	240

For the medium cooling rate system, Fig. 3e shows that both 10.3 Å and 10.5 Å tubes have a prominent phase transition at the temperature of nearly 260 K, whereas the smaller tube of 9.4 Å shows a higher temperature zone of the premature phase transition at around 275 K. However, there are generally more multiple peaks in the case of medium cooling rate than the fast cooling rate. This result means that ice structures are more slowly and gradually formed when cooling down in comparison with the fast cooling rate. The consistent ice structures are formed at temperatures lower than 260 K.

For the system with a slow cooling rate, there are even more multiple peaks compared with those faster cooling rates (Fig. 3f). The result means that the slower the cooling rate is, the more gradual and consistent ice structures are formed. While the small tube of 9.4 Å shows relatively resembled peaks, the systems of the bigger tubes show global peaks at both the high-temperature

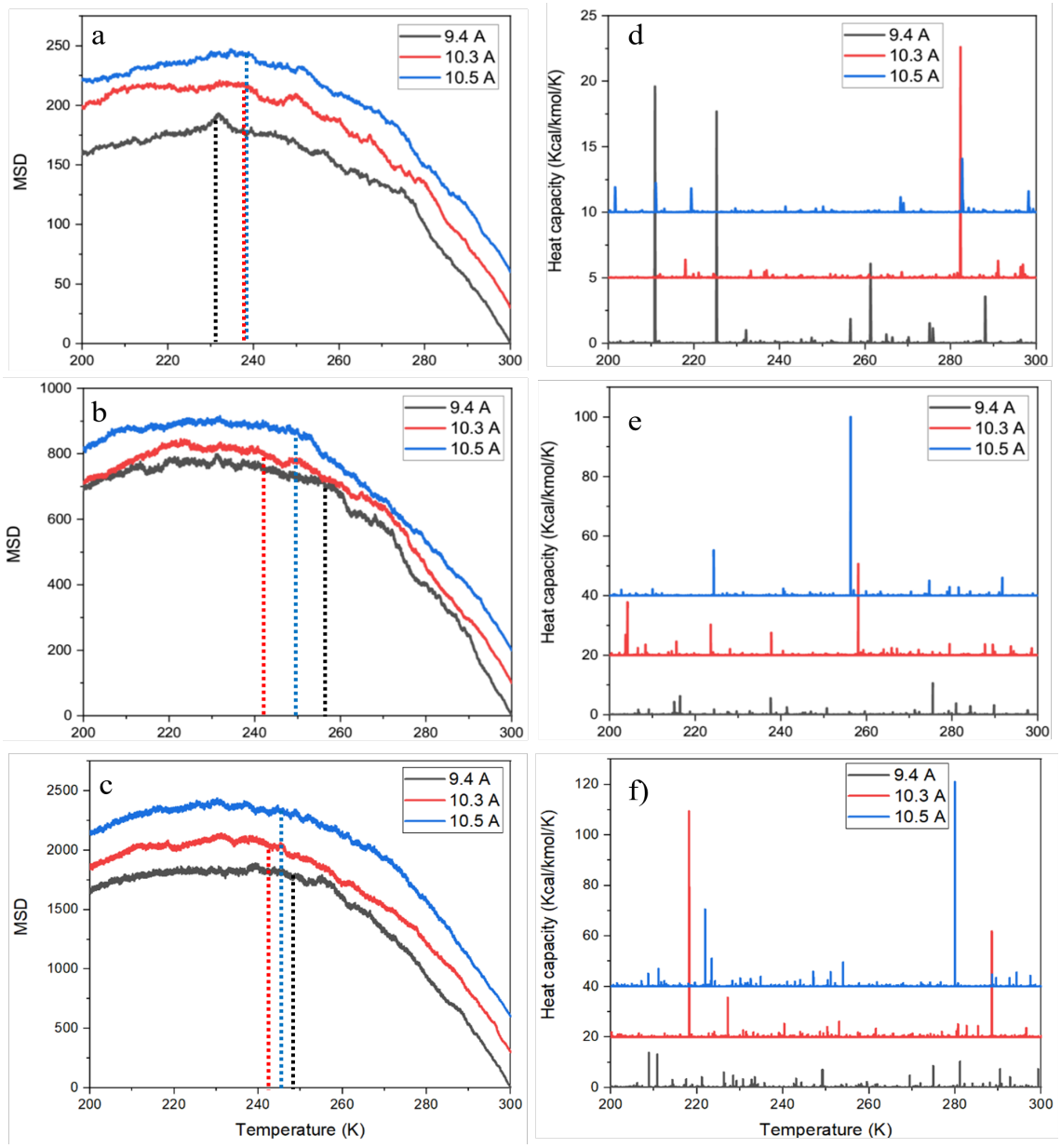

Fig. 3. (Color online) MSD-temperature (a-c) and heat capacity-temperature (d-f) graphs of water molecules after simulation for three different diameters of the carbon nanotubes, at 1 bar pressure. Graph a) and d) depict the fast cooling system, b) and e) belong to the medium cooling system, c) and f) belong to the slow cooling system. Dotted lines in the MSD graphs indicate the consistent ice formation point where the MSD lines become flat. Different line colors illustrate different tube diameters (9.4 Å is black, 10.3 Å is red, 10.5 Å is blue).

zone around 280 K and the low-temperature zone around 220 K. It is worth noticing that even the MSD graph (Fig. 3c) shows less motion of water molecules when the temperature reaches 240 K, the peak appearance around 220 K in Fig. 3f indicated that the solidification is still in progress. The results mean that there can exist both solid and liquid phases in the consistent ice structure, instead of the whole solid structure.

3.2. Under 2 bar pressure

Table 3. Summary of the noticeable phase transition points of systems under 2 bar pressure.

Cooling rate (K/s)	Diameter (Å)	Temperature of first local peak (K)	Critical phase transition point (K)
2×10^{11} (fast)	9.4	285	240
	10.3	285	235
	10.5	295	235
5×10^{10} (med)	9.4	285	230
	10.3	260	235
	10.5	295	240
$2 \times 10^{10}(slow)$	9.4	295	240
	10.3	290	240
	10.5	295	240

The systems at 2 bar show some different tendencies compared with the systems under 1 bar pressure. As shown in the MSD graphs (Figs. 4a - 4c), the ice formation behavior inside the SWCNT is somehow disturbed with raising the pressure. The critical points where the consistent ice structures are formed, are all lower than ones in the cases of 1 bar pressure, regardless of cooling rates. While the ice is gradually and continuously formed at the slow cooling rate under 1 bar pressure, that tendency happens at the medium cooling rate under 2 bar pressure. We hypothesize that the dual effect of extremely small space - high pressure slows down the stable solidification process of water in comparison with the systems at the lower pressures, yielding sufficiently smaller temperatures to form consistent ice. In another word, the higher pressure is, the lower of temperatures is for water to form consistent ice.

In addition, at 2 bar pressure (Fig. 4 and Table 3), the fast cooling rate makes a more rapid phase change in the water phase structures than the other cooling rates do, which is denoted by the spatial localization in the heat capacity graph (Fig. 4d). However, the peaks are majorly located at the high temperature above 290 K, except in the case of the 9.4 Å tube where the relatively high peaks are located in both high and low-temperature zones as similar as the system under 1 bar pressure.

Aside from that, the phase transition tendency undergoes a prominent change in the case of medium and slow cooling rates. In the case of the medium cooling rate, the ice formation is gradual

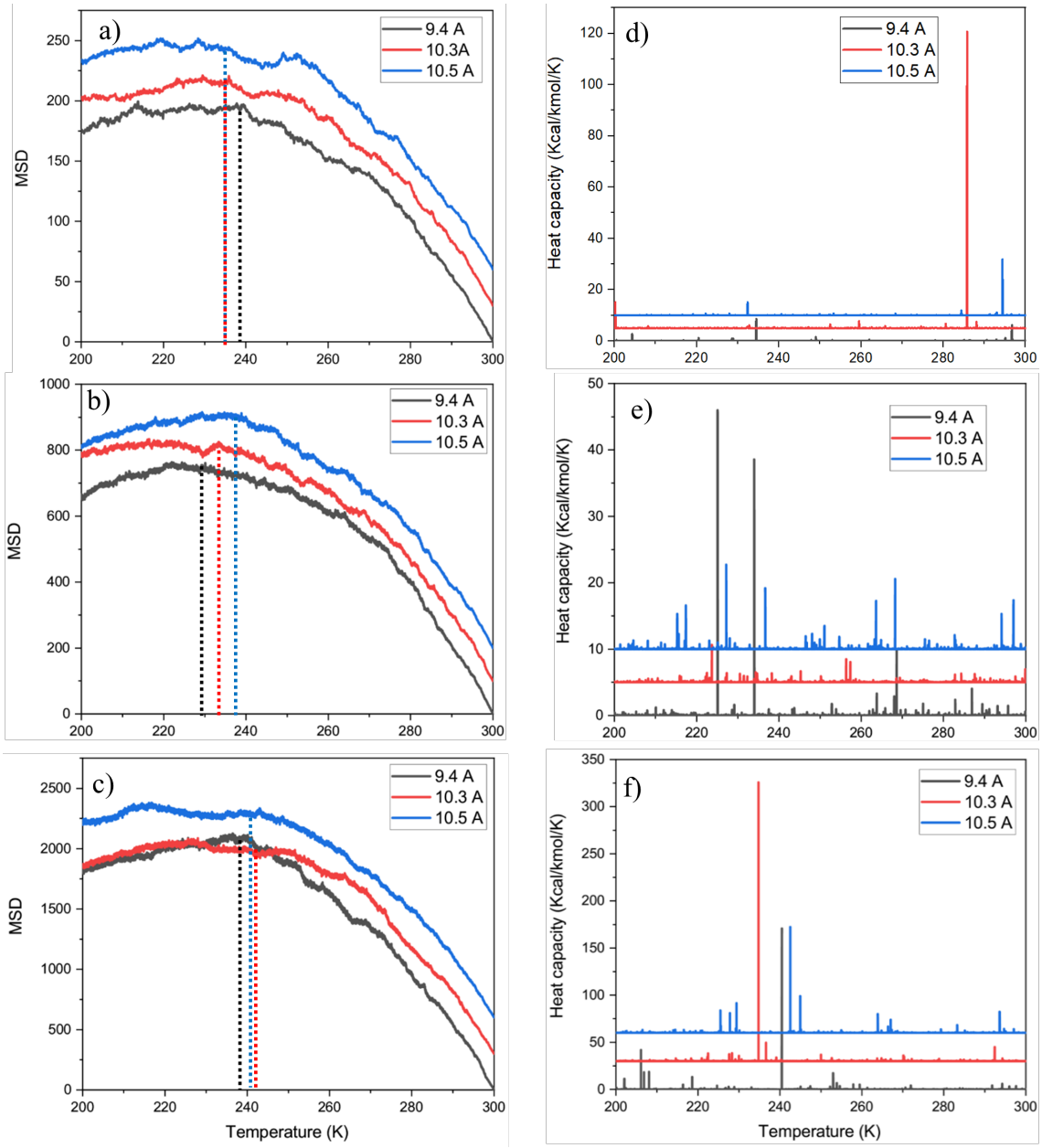

Fig. 4. MSD-temperature (a-c) and heat capacity-temperature (d-f) graphs of water molecules after simulation for three different diameters of carbon nanotubes, at 2 bar pressure. The order of graphs is the same as in Fig. 3.

and continuous, and we even observed that the global peaks in the heat capacity graph (Fig. 4e) are mostly distributed at temperatures lower than those in the systems under 1 bar pressure.

In the case of the slow cooling system, the heat capacity graph (Fig. 4f) shows a localization tendency that is different from the continuous tendency of the systems under 1 bar pressure. Those global peaks mostly lie in the range from 230 K to 250 K for all sizes of tubes. As we mentioned above, the lower temperatures to form the consistent ice means there is no major peak in the high-temperature zone. Furthermore, for the system with 9.4 Å tube, we observe a special case that the area where the major phase transition point overlaps with the sudden drop in the correspondent MSD graph, at around 240 K. The result indicates that there exists an extreme phase transition of water, where a liquid is immediately turned into the ice structure when raising the pressure and slowing down the cooling rate. That tendency of ice formation at such a low temperature has been observed previously for the system containing a carbon nanotube with the diameter of around 9.4 Å [5], and our result suggests that if the pressures are higher than the normal atmospheric pressure, that phenomenon may be eased even more.

3.3. Under 0.5 bar pressure

Table 4. Summary of the noticeable phase transition points of systems at 0.5 bar pressure.

Cooling rate (K/s)	Diameter (Å)	Temperature of first local peak (K)	Critical phase transition point (K)
2×10^{11} (fast)	9.4	285	230
	10.3	285	240
	10.5	290	245
5×10^{10} (med)	9.4	240	235
	10.3 295	240	
		10.5 295	245
2×10^{10} (slow)	9.4	~ 300	250
	10.3	285	235
	10.5	290	245

When the pressure dropped to 0.5 bar, the phase transition manifests a unique and more transparent tendency with the higher pressure, regardless of the cooling rates. This indicates the fact that lower pressure may lead to more intensive and sudden phase transition of water inside the SWCNT. The MSD graphs (Fig. 5a - 5c) show higher temperature critical points where the consistent ice may form, compared with the higher pressures regardless of the cooling rates. Especially, while the systems containing the larger tube of 10.3 Å and 10.5 Å have the MSD lines plateauing after the critical phase transition points, the systems of 9.4 Å tube show a sudden drop after the critical point when cooling at rates faster than 5×10^{10} K/s (as shown with a dotted line in Fig. 5a - 5b). The tendency is as similar to the 9.4 Å tube system under 2 bar and slow cooling rate conditions. The result implies that the small SWCNTs may facilitate an extreme phase transition of the water inside with sufficiently low pressure and fast cooling rate conditions.

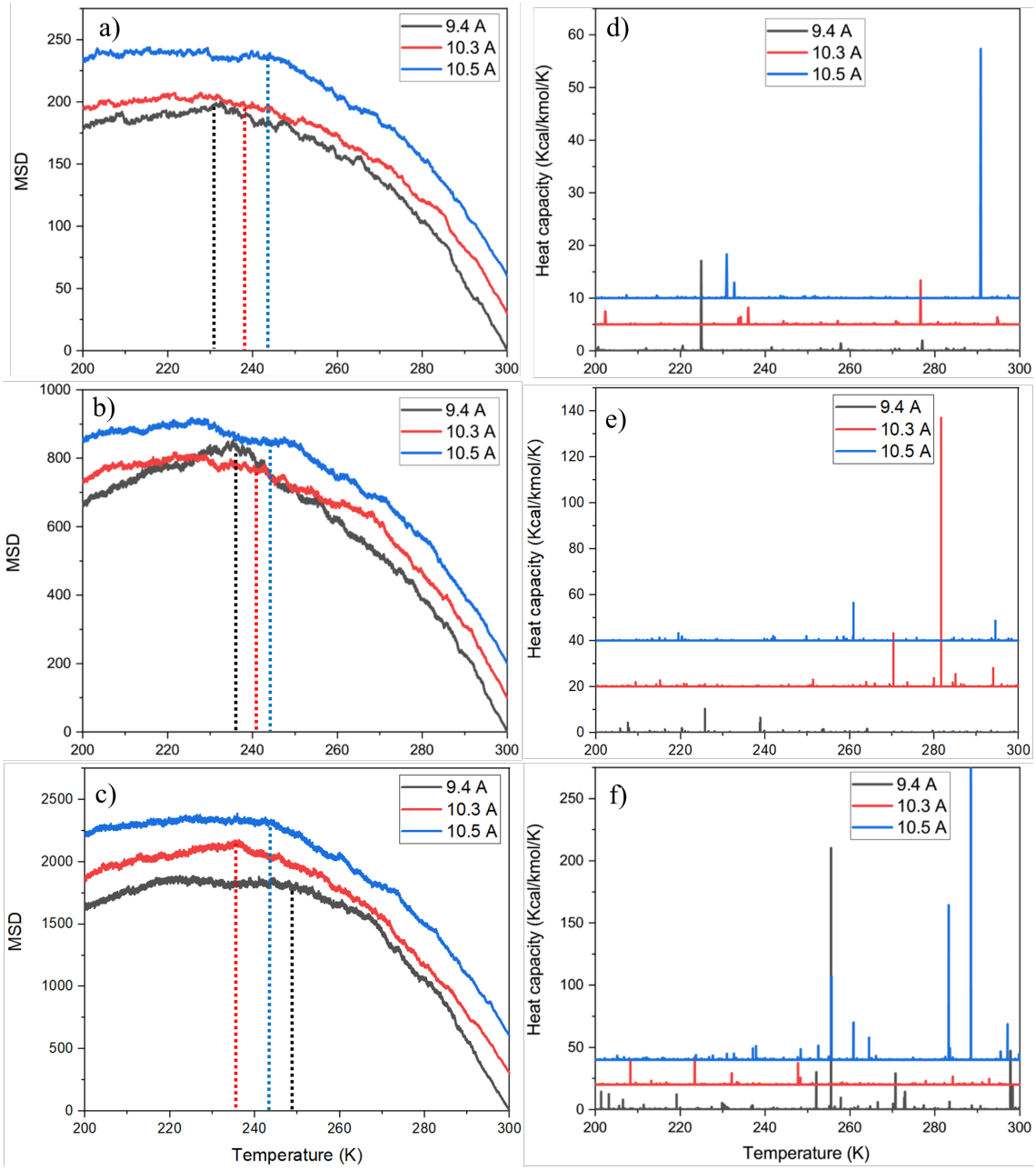

Fig. 5. MSD-temperature (a-c) and heat capacity-temperature (d-f) graphs of water molecules after simulation for three different diameters of carbon nanotubes, at 0.5 bar pressure. The order of graphs is the same as in Fig. 3.

More specifically, all heat capacity graphs show fewer peaks than the ones at the higher pressures (Fig. 5). That implies the fact that under the low pressures, disruptive phase transitions

of water inside the SWCNT are likely to happen instead of gradual phase transitions as in the systems under higher pressures.

As shown in the heat capacity data and Table 4, for the fast cooling rate, the systems of the bigger tubes (10.3 Å and 10.5 Å) show the major phase transition of the ice at high temperatures, ranging from 280 K to 290 K (Fig. 5d). However, in the case of the 9.4 Å tube, the system shows the major phase transition at the lower temperature around 230K, which corresponds to the extreme phase transition point in the MSD graph (Fig. 5a). In the case of the medium cooling system (Fig. 5e), the systems of 10.3 Å and 10.5 Å tubes show the major phase transitions at the high temperatures ranging from 260 K to 290 K. For the small tube of 9.4 Å, the peaks distribute at lower temperatures ranging from 220 K to 240 K, and they correspond to the extreme phase transition in the MSD graph as well. The results again show the same tendency as the previous study [5].

For the slow cooling systems, when compared with the fast and medium cooling rate systems under 0.5 bar pressure, the phase transition tendency is shifted to the gradual phase transition for all tube sizes with more appearance of multiple peaks (Fig. 5f). However, the consistent ice forming temperatures are all in higher temperature zones in comparison with the respective systems under the higher pressures. The result confirms that high pressures may drop the critical phase transition points of water inside the SWCNT. In detail, the biggest tube of 10.5 Å shows the major phase transition in the high temperature- zone between 280 K and 290 K. Meanwhile, the smallest tube system of 9.4 Å has the phase transition temperatures at around 255 K. For the 10.3 Å tube system, the solidification occurs at the lower temperatures (below 250 K) compared with the other tube sizes.

4. Conclusion

In general, we found two tendencies of the water solidification inside the SWCNT under different conditions:

1. The water phase transition depends prominently on the cooling rates. More specifically, when slowing down the cooling rate, the ice structure inside the SWCNT undergoes a more gradual phase transition (multiple peaks in the heat capacity graph). It means that at the fast cooling rate, the solidification phenomenon of water is more dramatic and inhomogeneous.

2. Changing the ambient pressure can make the phase transitions of water inside the SWCNT more dramatic when the cooling rate is sufficiently rapid. The high pressures prefer the gradual freezing processes, while the low pressures prefer the disruptive freezing processes.

However, there are some special cases of those systems above that are unsystematic when changing the conditions. The reason may come from the limited access to the proper force field as mentioned in Ref [1]. Thus, further research about the force fields of the water inside the SWCNT will be considered deeply in future work to get more consistent results.

Acknowledgement

We acknowledge Ho Chi Minh City University of Technology (HCMUT), VNU-HCM for supporting this study.

Conflict of interest

The authors declare that they have no competing financial interests.

References

[1] K. V. Agrawal, S. Shimizu, L. W. Drahushuk, D. Kilcoyne and M. S. Strano, *Observation of extreme phase transition temperatures of water confined inside isolated carbon nanotubes*, Nat. Nanotechnol. **12** (2017) 267.

[2] K. Koga, G. T. Gao, H. Tanaka, X. C. Zeng, *Formation of ordered ice nanotubes inside carbon nanotubes*, Nature **412** (2001) 802

[3] J. H. Walther, K. Ritos, E. R. Cruz-Chu, C. M. Megaridis and P. Koumoutsakos, *Barriers to superfast water transport in carbon nanotube membranes*, Nano Lett. **13** (2013) 1910.

[4] D. Takaiwa, I. Hatano, K. Koga and H. Tanaka, *Phase diagram of water in carbon nanotube*, Proc. Natl. Acad. Sci. **105** (2008) 39.

[5] J. Shiomi, T. Kimura and S. Maruyama, *Molecular dynamics of Ice-nanotube formation inside carbon nanotubes*, J. Phys. Chem. C **111** (2007) 12188.

[6] Y. Maniwa, H. Kataura, M. Abe, S. Suzuki, Y. Achiba, H. Kira and K. Matsuda, *Phase transition in confined water inside carbon nanotubes*, J. Phys. Soc. Jpn. **71** (2002) 2863.

[7] M. Yutaka, K. Hiromichi, A. Masatoshi, A. Udaka, S. Suzuki, Y. Achiba, H. Kira, K. Matsuda, H. Kadowaki and Y. Okabe, *Ordered water inside carbon nanotubes: formation of pentagonal to octagonal ice-nanotubes*, Chem. Phys. Lett. **401** (2005) 534.

[8] J. Bai, J. Wang and X. C. Zeng, *Multiwalled ice helixes and ice nanotubes*, Proc. Natl. Acad. Sci. **103** (2006) 19664.

[9] T. Ohba, S. I. Taira, K. Hata, K. Kanekoc and H. Kanoh *Predominant nanoice growth in single-walled carbon nanotubes by water-vapor loading*, RSC Adv. **2** (2012) 3634.

[10] A. I. Kolesnikov, J. M. Zanotti, C. K. Loong, P. Thiyagarajan, A. P. Moravsky, R. O. Loutfy and C. J. Burnham *Anomalously soft dynamics of water in a nanotube: A revelation of nanoscale confinement*, Phys. Rev. Lett. **93** (2004) 035503.

[11] K. Matsuda, T. Hibi, H. Kadowaki, H. Kataura and Y. Maniwa, *Water dynamics inside single-wall carbon nanotubes: NMR observations*, Phys. Rev. B **74** (2006) 073415.

[12] H. Kyakuno, K. Matsuda, H. Yahiro, Y. Inami, T. Fukuoka, Y. Miyata, K. Yanagi, Y. Maniwa, H. Kataura, T. Saito, M. Yumura and S. Iijima, *Confined water inside single-walled carbon nanotubes: Global phase diagram and effect of finite length*, J. Chem. Phys. **134** (2011) 244501.

[13] V. V. Hoang, Cooling rate effects on structure of amorphous graphene, Phys. B Condens. Matter 456 (2015) 50.

[14] V. Van Hoang and N.T. Long, *Amorphous silicene - a view from molecular dynamics simulation*, J. Phys. Condens. Matter **28** (2016) 19540.

[15] N. H. Giang and V. V. Hoang, *Influences of cooling rate on formation of amorphous germanene*, Physica E: Low-dimensional Systems and Nanostructure **126** (2021) 114492.

[16] W. Humphrey, A. Dalke and K. Schulten, *VMD molecular dynamics*, J. Molec. Graphics **14** (1996) 33.

[17] L. Martínez, R. Andrade, E. G. Birgin and J. M. Martínez, *Packmol: A package for building initial configurations for molecular dynamics simulations*, J. Comput. Chem. **30** (2009) 2157.

[18] A.D. MacKerell Jr, D. Bashford, M. L. D. R. Bellott, R. L. Dunbrack Jr, J. D. Evanseck, M. J. Field, S. Fischer, J. Gao, H. Guo, S. Ha, D. Joseph-McCarthy, L. Kuchnir, K. Kuczera, F. T. K. Lau, C. Mattos, S. Michnick, T. Ngo, D. T. Nguyen, B. Prodhom, W. E. Reiher, B. Roux, M. Schlenkrich, J. C. Smith, R. Stote, J. Straub, M. Watanabe, J. Wiórkiewicz-Kuczera, D. Yin, and M. Karplus, *All-atom empirical potential for molecular modeling and dynamics studies of proteins*, J. Phys. Chem. **102** (1998) 3586.

[19] S. Stuart, A. B. Tutein and J. Harrison, *A reactive potential for hydrocarbons with intermolecular interactions*, J. Chem. Phys. **112** (2000) 6472.

[20] M. Raju, A. V. Duin and M. Ihme, *Phase transitions of ordered ice in graphene nanocapillaries and carbon nanotubes*, Sci. Rep. **8** (2018) 3851.